PHYSICAL REVIEW A VOLUME 42, NUMBER 3 1 AUGUST 1990

Rapid Communications

The Rapid Communications section is intended for the accelerated publication of important new results. Since manuscripts submitted to this section are given priority treatment both in the editorial office and in production, authors should explain in their submittal letter why the work justifies this special handling. A Rapid Communication should be no longer than 3½ printed pages and must be accompanied by an abstract. Page proofs are sent to authors.

Doubly excited states in electron-impact ionization of C^{3+} ions

S. S. Tayal
Department of Physics and Astronomy, Louisiana State University, Baton Rouge, Louisiana 70803

Ronald J. W. Henry
Department of Physics, Auburn University, Auburn, Alabama 36849

(Received 2 April 1990)

Resonances due to the resonant-excitation–double-autoionization process in the electron-impact ionization of C^{3+} ions are calculated using the R-matrix method. Twelve autoionizing states arising from the $1s2s^2$, $1s2s2p$, $1s2p^2$, $1s2s3s$, $1s2s3p$ configurations, together with the ground $1s^22s\,^2S$ and excited $1s^22p\,^2P^o$, $1s^23s\,^2S$, $1s^23p\,^2P^o$, $1s^23d\,^2D$ states, are included in the close-coupling expansion. These states are represented by accurate configuration-interaction wave functions. The present results are in good agreement with the recent crossed-beam measurement.

Müller *et al.*[1] recently presented unambiguous experimental evidence for the fine resonance structures arising from the resonant-excitation–double-autoionization (REDA) and resonant-excitation–auto-double-ionization (READI) processes in electron-impact ionization of Li-like C^{3+} ions. In both of these processes the incident electron is captured temporarily with simultaneous excitation of an inner-shell electron to form a doubly excited state of the ion which then can decay either by sequential emission or by simultaneous emission of two electrons. These are resonant processes that can make significant contributions to the electron-impact single-ionization cross section. The excitation-autoionization (EA) process is another important indirect physical mechanism for ionization which received considerable theoretical and experimental attention in recent years. It is a nonresonant process in which an inner-shell electron is excited to a level above the ionization threshold with subsequent autoionization. The inner-shell excitation can cause a significant rise in the ionization cross section close to the threshold for the excitation process.

The REDA process was first described by LaGattuta and Hahn[2] in connection with the electron-impact ionization of Na-like Fe^{15+} ions and it gives rise to resonances below the autoionizing states. Some evidence of these resonances in electron-impact ionization of Fe^{15+} was obtained by Gregory *et al.*[3] However, the results of their measurement did not support the predicted large contribution of the REDA process. We performed a close-coupling calculation to obtain the contributions of EA and REDA processes to electron-impact ionization cross sections of Fe^{15+} ions.[4] Our results are in good agreement with the crossed-beam measurement of Gregory *et al.*[3] More recently, Chen, Reed, and Moores[5] calculated the REDA cross sections for Fe^{15+} using a multiconfiguration Dirac-Fock model. They found that the contributions of REDA to the ionization cross section of Fe^{15+} is about 30%. The READI process was suggested by Henry and Msezane[6] as a possible indirect process of ionization and Pindzola and Griffin[7] calculated its contribution to the electron-impact ionization of Li-like ions using the first- and second-order perturbation theory. Their calculation predicted very small cross sections for the READI process.

Electron-impact ionization cross sections for positive ions are of fundamental importance in the analysis of astrophysical and laboratory plasmas. The relative simplicity of the structure of C^{3+} ions and the availability of accurate high-resolution data motivated us to carry out a detailed close-coupling calculation for the contributions of REDA and EA processes to the electron-impact ionization of C^{3+} ions. There has been considerable theoretical and experimental interest in the studies of electron-impact ionization of Li-like ions during the past several years. In addition to the recent measurements of Müller *et al.*[1] for C^{3+}, Crandall *et al.*[8] reported electron-impact ionization cross sections for B^{2+} and O^{5+} ions and Crandall *et al.*[9] measured cross sections for electron-impact ionization of C^{3+}, N^{4+}, and O^{5+} ions. On the theoretical side, Henry[10] calculated contributions of the EA process to the electron-impact ionization of C^{3+}, N^{4+}, and O^{5+} ions in a six-state close-coupling approximation. Jakubowicz and Moores[11] calculated electron-impact ionization cross sections for Li-like ions using the Coulomb-Born exchange and distorted-wave exchange approximations. They represented the initial and final states of the target ions by close-coupling wave functions. This approach allows the inclusion of complete Rydberg series of autoionizing

states in the calculation.

In the case of C^{3+} ions, the EA process can be written as

$$e^- + C^{3+}(1s^2 2s) \rightarrow e^- + C^{3+*}(1s2snl) \rightarrow C^{4+}(1s^2) + e^- , \quad (1)$$

while the REDA process is given by

$$e^- + C^{3+}(1s^2 2s) \rightarrow C^{2+**}(1s2snln'l') \rightarrow C^{3+*}(1s2snl) + e^- \rightarrow C^{4+}(1s^2) + e- . \quad (2)$$

The doubly excited state of the ion formed as a result of capture of the incident electron [Eq. (2)] can also decay by other pathways which do not contribute to net single ionization. For example, the doubly excited state of the C^{2+} ion can decay either by single autoionization to a bound state of C^{3+} ion giving rise to resonances in the electron-ion scattering process or alternatively, it can radiatively decay to a bound state of a C^{2+} ion leading to the familiar dielectronic recombination process. Thus in many cases the cross sections for the REDA process may depend on the branching ratios at each step in Eq. (2). For C^{3+} ions, the radiative decay rate is sufficiently small compared to the autoionization rate that unit branching ratios can be assumed. However, the question of autoionization of the $(N+1)$-electron state to a N-electron bound state which does not contribute to ionization or to a N-electron autoionization state which does contribute will be discussed below.

The total wave function representing the electron-ion collision is expanded as

$$\psi_k = A \sum_{i,j} c_{ijk} \Phi_i(1,2,3;\hat{r}_4\sigma_4) u_{ij}(r_4) r_4^{-1} + \sum_j d_{jk} \phi_j(1,2,3,4) , \quad (3)$$

where A is the antisymmetrization operator, the Φ_i are channel functions formed by coupling the spin and angular functions of the scattered electron with the target-state wave functions, ϕ_j are bound-state-type functions, and u_{ij} are the numerical basis functions describing the radial motion of the scattered electron. The coefficients c_{ijk} and d_{jk} are determined by diagonalizing the total Hamiltonian of the $(N+1)$-electron system. In order to account accurately for the process in which the incident electron is captured into a compound state of the C^{3+} ion plus incident electron, we have included a large number of bound terms of the appropriate symmetry in the second expansion in Eq. (3). We included the ground $1s^2 2s\ ^2S$ and excited $1s^2 2p\ ^2P^\circ$, $1s^2 3s\ ^2S$, $1s^2 3p\ ^2P^\circ$, $1s^2 3d\ ^2D$ bound states together with the twelve autoionizing states arising from the $1s2s^2$, $1s2s2p$, $1s2p^2$, $1s2s3s$, and $1s2s3p$ configurations in the first expansion in Eq. (3). These target states are represented by configuration-interaction (CI) wave functions constructed from the six orthogonal one-electron orbitals: $1s$, $2s$, $2p$, $3s$, $3p$, and $3d$. The $1s$ and $2s$ radial functions are those of the $1s^2 2s\ ^2S$ ground state given by Clementi and Roetti.[12] The $2p$ function is optimized on the combination of

$$1s2s(^3S)2p\ ^2P^\circ + 1s2s(^1S)2p\ ^2P^\circ$$

and the $3s$ and $3p$ orbitals are chosen to improve the energies of $1s2s(^3S)3s\ ^2S$ and $1s2s(^3S)3p\ ^2P^\circ$ excited states, respectively. Finally, the $3d$ function is optimized on the excited $1s^2 3d\ ^2D$ state. In Table I we give the calculated excitation energies in eV where they are compared with the experiment and other calculation. We used 11, 10, 4, and 3 configurations for the description of the ^2S, $^2P^\circ$, ^2D, and ^2P states, respectively, while 4, 3, and 2 configurations are used to describe $^4P^\circ$, ^4P, and ^4S states, respectively. The CI wave functions are also used to calculate the absorption oscillator strengths for the dipole-allowed transitions between the ground and autoionization states. The length and velocity values of oscillator strengths are listed in Table II. The good agreement between the length and velocity forms of oscillator strengths provides confidence in the accuracy of the target wave functions.

Application of a variational principle leads to a set of coupled integrodifferential equations which are solved numerically by the R-matrix method.[13] Twenty-five continuum orbitals of each angular symmetry are included, giving good convergence in the energy range of interest. The largest number of channels included in the present work is 28. At each electron energy results are obtained for six values of angular momenta $L = 0$–5. These partial waves gave converged cross sections for all the transitions. The total ionization cross section can be assumed as the sum of direct and indirect ionization processes, if the interference between these processes is ignored. Crandall *et al.*[8] have argued that the interference effects did not make appre-

TABLE I. Excitation energies (eV) of C^{3+} states relative to the ground state.

State	Energy		
	Present	Experiment[a]	Other calculation[b]
$1s^2 2s\ ^2S$	0.0	0.0	0.0
$1s^2 2p\ ^2P^\circ$	8.74	8.00	
$1s^2 3s\ ^2S$	37.55	37.55	
$1s^2 3p\ ^2P^\circ$	39.98	39.68	
$1s^2 3d\ ^2D$	40.19	40.28	
$1s2s^2\ ^2S$	292.86		293.6
$1s2s2p\ ^4P^\circ$	295.28		296.9
$1s2s(^1S)2p\ ^2P^\circ$	300.78		301.8
$1s2p^2\ ^4P$	303.24		
$1s2s(^3S)2p\ ^2P^\circ$	305.09		306.8
$1s2p^2\ ^2D$	307.66		
$1s2p^2\ ^2P$	308.40		
$1s2p^2\ ^2S$	314.12		
$1s2s3s\ ^4S$	335.22		336.1[c]
$1s2s(^3S)3s\ ^2S$	336.53		336.1[c]
$1s2s3p\ ^4P^\circ$	337.88		338.2[c]
$1s2s(^3S)3p\ ^2P^\circ$	338.80		338.2[c]

[a]Reference 16.

[b]Reference 7.

[c]Center-of-gravity energies.

TABLE II. Oscillator strengths for dipole-allowed transitions.

Transition	Present calculation f_L	f_V
$1s^2 2s\ ^2S \rightarrow 1s2s(^1S)2p\ ^2P^\circ$	0.50	0.48
$1s^2 2s\ ^2S \rightarrow 1s2s(^3S)2p\ ^2P^\circ$	0.14	0.14
$1s^2 2s\ ^2S \rightarrow 1s2s(^3S)3p\ ^2P^\circ$	0.088	0.083

ciable contribution to the electron-impact ionization of Li-like ions. We obtained total ionization cross section by the relation

$$\sigma_{\text{tot}} = \sigma_{\text{direct}} + \sum_j \sigma^j_{\text{excit}} B^q_j , \tag{4}$$

where σ_{direct} is the direct ionization cross section, σ^j_{excit} is the excitation cross section to the j autoionizing state, and B^q_j is the branching ratio for autoionization from the level j which is assumed to be unity in the present work. The direct-ionization cross sections for Li-like ions are calculated by Younger in a distorted-wave exchange approximation.[14] We renormalized Younger's result for C^{3+} ions by a factor of 0.80.

Electron-impact ionization cross sections for C^{3+} are given in Fig. 1. The present results are shown by the solid curve and the dashed curve gives the renormalized direct-ionization cross sections obtained by using Younger's parameters.[14] The crossed-beam experimental data of Müller *et al.*[1] are shown by the dotted curve. We considered twelve autoionizing states having threshold energies between 292.86 and 338.80 eV in this work. Our calculation shows resonance structure due to the REDA process in this energy region. These resonances occur as Rydberg series below the autoionization states included in the close-coupling expansion. In order to delineate the resonance structure in our calculation, the inner-shell excitation cross sections are calculated at 1779 energy points using a fine energy mesh (0.0272 eV) in the threshold region. The cross sections are then convoluted with a 2.0-eV full-width-at-half-maximum Gaussian to simulate experimental energy spread. In order to match approximately the calculated position of first dominant resonance feature in the cross section with the experiment, the theoretical energy scale is adjusted to the lower-energy side by 2.0 eV. This adjustment is occasioned by the use of approximate wave functions and an incomplete account of correlation effects in the representation of target states. It is clear from the figure that our calculation reproduces well the various features in the cross section in the threshold region. However, there are some discrepancies in magnitude and trend of the cross sections. The calculated results of cross section in the $1s2s2l$ threshold region are larger than the measured values, while in the $1s2s3l$ threshold region the present results are lower than the measurement. There is an increasing trend of measured cross sections for C^{3+} at higher electron energies which is not noted in experiments on other Li-like ions. Hofmann *et al.*[15] attribute this different behavior of the C^{3+} cross sections to the uncertainty in normalization.

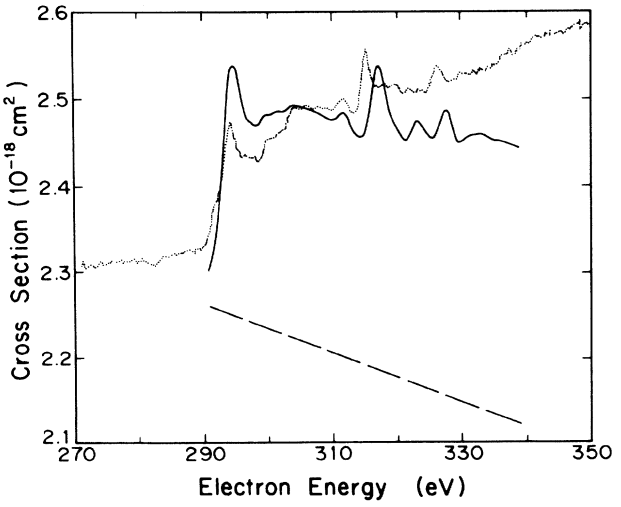

FIG. 1. Electron-impact ionization cross section for the ground $1s^2 2s\ ^2S$ state of C^{3+} ions. Solid curve, cross sections from this work; dashed curve, distorted-wave direct-ionization cross sections (Ref. 14); dotted curve, measures cross sections (Ref. 1).

The inner-shell excitation cross sections for the $^2S \rightarrow 1s2s2p\ ^4P^\circ$ and $^2S \rightarrow 1s2s(^1S)2p\ ^2P^\circ$ transitions make dominant contributions in the threshold region. The cross sections are fairly smooth in the $1s2p^2$ threshold region. There are no resonances in this energy region since two bound electrons are excited. However, just below $1s2p^2\ ^2S$ threshold there is a peak and a dip in the cross sections. This is due to the presence of resonances in this energy region which belong to the $1s2s3ln'l'$ Rydberg series converging to the $1s2s3l$ thresholds. These resonances happen to lie below the $1s2p^2\ ^2S$ threshold where they interfere with the smooth background cross sections in this region. Our calculation shows strong resonance features around 315 and 326 eV in the $1s2s3l$ threshold region, in agreement with the measurement. The calculated positions of these peaks are shifted to the higher energy. The calculation also predicts a fairly strong feature between these two peaks which is not as clearly visible in

TABLE III. Calculated inner-shell excitation cross sections (10^{-18} cm^2) from the ground $1s^2 2s\ ^2S$ state.

Upper state	Cross sections 340 eV	350 eV	360 eV
$1s2s^2\ ^2S$	0.0272	0.0262	0.0258
$1s2s2p\ ^4P^\circ$	0.0770	0.0732	0.0697
$1s2s(^1S)2p\ ^2P^\circ$	0.0948	0.0983	0.1018
$1s2p^2\ ^4P$	0.0025	0.0023	0.0020
$1s2s(^3S)2p\ ^2P^\circ$	0.0565	0.0557	0.0552
$1s2p^2\ ^2D$	0.0026	0.0026	0.0018
$1s2p^2\ ^2P$	0.0020	0.0020	0.0019
$1s2p^2\ ^2S$	0.0081	0.0114	0.0189
$1s2s3s\ ^4S$	0.0025	0.0024	0.0022
$1s2s(^3S)3s\ ^2S$	0.0065	0.0055	0.0048
$1s2s3p\ ^4P^\circ$	0.0066	0.0060	0.0056
$1s2s(^3S)3p\ ^2P^\circ$	0.0176	0.0176	0.0158
Total	0.1025	0.1025	0.1069

the measurement. In the investigation of the C^{3+} ionization cross section, we initially performed a 13-state close-coupling calculation in which the same states as in the 17-state close-coupling calculation were retained except for $1s^22p$, $1s^23s$, $1s^23p$, and $1s^23d$. We obtained a fairly strong resonance feature in the 301-eV range associated with $1s2s2pnl$ Rydberg series. This feature is not present in the measurements. It is an artifact of the thirteen-state theoretical model in that in this energy range the only mechanism for loss of flux is excitation to $1s2s^2$ or $1s2s2p$. By including $1s^22p$ and $1s^23l$ states, other channels are available for loss of energy and the resonance contribution is significantly decreased. Autoionization to N-electron bound states $1s^2nl$ may be important decay channels. This is demonstrated by the inclusion of $nl=2p$, $3s$, $3p$, and $3d$. Even higher excited bound states may still be important. This will be the subject of future investigations. At present, apart from the above feature, the thirteen- and seventeen state results are essentially the same over the energy range 290–340 eV.

In Table III, we have listed cross sections for excitation of twelve autoionizing states at incident electron energies 340, 350, and 360 eV. In this energy region, our calculations do not include REDA contributions. It can be easily seen that the $^2S\rightarrow 1s2s(^1S)2p\,^2P^\circ$ transition makes the largest contribution which increases with the increase in energy. It should be noted that we did not include higher inner-shell excited states in the present calculation which will also contribute to the EA process in this energy region.

In conclusion, we have presented the calculation of REDA and EA processes in electron-impact ionization of Li-like C^{3+} ions. The calculated features in the cross sections are in good agreement with the new crossed-beam experiment. There are some discrepancies in the magnitude of the cross sections at the peaks as well as at higher energies. The calculated peaks are shifted to higher energy due to the difference in calculated and measured excitation thresholds. The C^{3+} ion is one of the simplest atomic systems where inner-shell excitation is possible and in which relativistic effects and radiative decay of autoionizing states can be ignored.

This research is supported in part by the U.S. Department of Energy, Division of Chemical Sciences. The authors wish to thank Dr. M. S. Pindzola and Dr. N. Badnell for discussion and information concerning radiative and autoionization rates.

[1]A. Müller, G. Hofmann, K. Tinschert, and E. Salzborn, Phys. Rev. Lett. **61**, 1352 (1988).

[2]K. J. LaGattuta and Y. Hahn, Phys. Rev. A **24**, 2273 (1981).

[3]D. C. Gregory, L. J. Wang, F. W. Meyer, and K. Rinn, Phys. Rev. A **35**, 3256 (1987).

[4]S. S. Tayal and R. J. W. Henry, Phys. Rev. A **39**, 3890 (1989).

[5]M. H. Chen, K. J. Reed, and D. L. Moores, Phys. Rev. Lett. **64**, 1350 (1990).

[6]R. J. W. Henry and A. Z. Msezane, Phys. Rev. A **26**, 2545 (1982).

[7]M. S. Pindzola and D. C. Griffin, Phys. Rev. A **36**, 2628 (1987).

[8]D. H. Crandall, R. A. Phaneuf, D. C. Gregory, A. M. Howald, D. W. Mueller, T. J. Morgan, G. H. Dunn, D. C. Griffin, and R. J. W. Henry, Phys. Rev. A **34**, 1757 (1986).

[9]D. H. Crandall, R. A. Phaneuf, B. E. Hasselquist, and D. C. Gregory, J. Phys. B **12**, L249 (1979).

[10]R. J. W. Henry, J. Phys. B **12**, L309 (1979).

[11]H. Jakubowicz and D. L. Moores, J. Phys. B **14**, 3733 (1981).

[12]E. Clementi and C. Roetti, At. Data Nucl. Data Tables **14**, 177 (1974).

[13]K. A. Berrington, P. G. Burke, M. LeDourneuf, W. D. Robb, K. T. Taylor, and Vo Ky Lan, Comput. Phys. Commun. **23**, 233 (1981).

[14]S. M. Younger, J. Quant. Spectrosc. Radiat. Transfer **26**, 329 (1981); Phys. Rev. A **22**, 111 (1980).

[15]G. Hofmann, A. Müller, K. Tinschert, and E. Salzborn, Z. Phys. D **16**, 113 (1990).

[16]C. E. Moore, *Atomic Energy Levels,* Natl. Bur. Stand. Ref. Data Ser., Natl. Bur. Stand. (U.S.) Circ. No. 35 (U.S. GPO, Washington, DC, 1971), Vol. 1.